Transportation Geotechnics 17 (2018) 133–140

Contents lists available at ScienceDirect

Transportation Geotechnics

journal homepage: www.elsevier.com/locate/trgeo

Two-staged kinetics of moduli evolution with time of a lime treated soil under different curing temperatures

Jacinto Silva[a], Miguel Azenha[a], A. Gomes Correia[a,*], Bertrand François[b]

[a] University of Minho, ISISE, Portugal
[b] Université Libre de Bruxelles, BATir, Belgium

ARTICLE INFO

Keywords:
Soil treatment
Wave propagation
Stiffness
Temperature effects
Activation energy
Modelling

ABSTRACT

This paper addresses the temperature effects on the kinetics of moduli evolution with time of a silty soil treated with quicklime. The moduli were obtained using different laboratory wave propagation test methods (UPV-ultrasonic pulse velocity, PZT-piezoelectric transducers, EMM-ARM-elasticity modulus measurement based on ambient response method) and unconfined cyclic compression tests with on-specimen deformation measurements. This experimental work was first carried out under a reference curing temperature of 30 °C, allowing the comparison of results obtained by the different test methods, as well as the identification of two stages on the modulus evolutions with time. These two stages were also revealed on additional EMM-ARM tests at 20 °C and 40 °C. These stages were tentatively explained by two different chemical phenomena and described by a mathematical model integrating two different activation energies. The findings of this work show the potential of using EMM-ARM to estimate the activation energies helping the modelling of temperature effects on the E-modulus evolution with time of complex soil-lime mixtures.

Introduction

The mixture of small quantities of chemical binders, such as lime, can improve significantly the strength and stiffness of fine grained soils to suit the engineering needs of construction projects, often resulting in cost savings and other tangible benefits for both the project and the owner [1–3]. This improvement effect on mechanical properties is generally observed in two distinct stages: the first is considered to occur over the few days immediately after mixing and the second can start days or weeks later and can be observed over long periods of time [4–6]. The soil treatment with lime consists of adding and mixing lime with soil in presence of water, resulting in several physicochemical modifications of the soil, such as: cationic exchange, flocculation, carbonation and pozzolanic reaction [7,8]. As result of these processes, some modifications on the geotechnical characteristics of the soil can be observed, as improvement in terms of plasticity, workability, shear strength, stiffness, swelling, compressibility, durability and soil compaction characteristics [9–11]. During the cationic exchange, the lime can be fixed by the available clay minerals and thus becomes unavailable for other reactions, as pozzolanic reactions [7]. However, if there is an excess of lime, then other chemical reactions will occur. In particular, it can contribute to a highly alkaline pH (above 12) promoting the release of silica and aluminates of the available clay particles [12]. These materials, also called pozzolans, are able to react with calcium ions (pozzolanic reactions) resulting in the formation of calcium aluminates hydrates (CAH) and calcium silicates hydrates (CSH) which provide higher strength and stiffness of the soil [7,8,13]. These reactions are usually slow at curing temperatures of 20 °C and can occur for a long periods of time and yield various amorphous phases (gels) [8]. However, it is noticeable that the increase of curing temperature has a dramatic effect on these reactions, particularly at temperatures above 30 °C [7]. In fact, this effect of temperature is frequently used to accelerate these reactions and to reduce the duration of some laboratory studies, as the qualification of additives, as fly ash and other pozzolans [14].

Despite the extensive studies concerning the soil treatment with lime there are some issues that have not yet been thoroughly addressed, namely the quantification of the temperature influence on the soil-lime reactions with specific focus on their corresponding activation energies. This quantification could be interesting to predict the in-situ evolution of the mechanical properties, as strength and/or stiffness, of a lime treated soil layer based on the actual temperature history and stiffness evolution determined in laboratory at reference temperature.

This paper presents the results of a joint study of the temperature effects on the stiffness evolution of a silt soil treated with quicklime, performed in collaboration between the University of Minho (UM –

* Corresponding author.
E-mail address: agc@civil.uminho.pt (A. Gomes Correia).

https://doi.org/10.1016/j.trgeo.2018.09.013
Received 9 June 2018; Received in revised form 21 September 2018; Accepted 29 September 2018
Available online 09 October 2018

Portugal) and Université Libre de Bruxelles (ULB – Belgium). The stiffness evolution of a soil-lime mixture cured at 30 °C is assessed by means of: wave propagation techniques, as piezoelectric sensors (PZT) and ultrasonic pulse velocity (UPV); unconfined cyclic compression (UCC) with local measurement of deformation and; elasticity modulus measurement based on ambient response method (EMM-ARM). The EMM-ARM allows the continuous measurement of the evolution of E-modulus of a given sample, placed in a testing mould under known support conditions [15]. It relies on naturally occurring vibrations to excite the tested sample, infer its first resonant frequency (based on the measurements of an accelerometer), and ultimately quantify the E-modulus of the tested material. Even though EMM-ARM was initially devised for concrete testing, it has been extensively applied (and validated) in the scope of stabilized soils by the research team at the University of Minho [16–19].

The kinetics of the stiffness evolution of the same mixture of lime treated soil cured at temperatures of 20 °C, 30 °C and 40 °C was assessed through EMM-ARM, in order to identify the activation energy of the stiffness build-up.

This study is considered pioneering both in the original combination of experimental techniques (PZT and EMM-ARM, for example), as well as to the research findings in assessing the effect of temperature on the kinetics of stiffness evolution of soils treated with lime.

Methods

Unconfined cyclic compression

Unconfined cyclic compression (UCC) tests, with on-specimen deformation measurement, were performed on cylindrical specimens with 100 mm diameter and 200 mm height, in order to quantify the E-modulus. The experimental procedure was based on the previous works of Gomes Correia [20] and Gomes Correia et al. [21,22]. The load equipment consisted in a 50 kN hydraulic actuator, which included a load cell. The deformations were measured by 3 displacement transducers (LVDTs) that were supported by 2 metallic rings, which were in turn attached to the tested specimen, as illustrated by Fig. 1.

Three continuous loading/unloading cycles, with a load rate of 50 N/s, were applied at several ages of testing. The maximum load applied was such that the maximum strain range was kept bellow 5×10^{-5}, which is considered to be in the very small strain domain, in accordance to existing studies with stabilized soils [23].

Wave propagation based techniques

Wave propagation techniques are frequently used for stiffness assessment of stabilized soils [24,25]. In fact, the compression wave velocity (V_P) and the bulk density (ρ) can be related with the maximum constrained modulus (M) using Eq. (1) based on the theory of wave propagation in an infinite elastic medium. V_P can be determined from the measurement of the travel time of the wave over a known distance between the transducers placed at each end of the specimen.

$$M = \rho \cdot V_p^2 \quad (1)$$

In the present work, two different techniques based on the measurement of compression wave propagation velocity were used: ultrasonic pulse velocity (UPV) and piezoelectric transducers (PZT). In both techniques, a predefined input wave is generated by the transmitter transducer, and then travels through the specimen, being finally received by the receiver transducer. The time required for the wave to propagate through the specimen is determined in the time domain by identifying the first deflection of the wave at the receiver transducer.

Ultrasonic pulse velocity – UPV

Ultrasonic pulse velocity (UPV) measurements were performed in cylindrical specimens with 46 mm in diameter and 70 mm long. The measurement equipment comprised a unit for signal generation and reception – the Proceq Pundit Lab [26] – connected to a personal computer with the software Punditlink [26], together with two 54 kHz circular transducers (transmitter/receiver). The tests were performed with a single pulse of sinusoidal signal with an input frequency of 54 kHz and signal amplitude of 500 V. During the test, the specimen was kept vertically with the transducers in contact at the extremities, as can be observed in Fig. 2. Conductive gel was used to ensure maximum coupling between the transducers and the specimen. The travel time of the compression wave was visually evaluated in time domain by measuring the instant of the first deflection of the wave.

Piezoelectric transducers – PZT

Measurements of wave propagation time were performed using ultrasonic piezoelectric sensors (PZT) on specimens with 36 mm in diameter and 71 mm long. The PZT sensors used were produced in the Civil Engineering laboratory at BATir, Université Libre de Bruxelles and consist on a very thin square ceramic patch with about 1 cm^2 where an electric cable was conductively glued on one side, as depicted in Fig. 3.

PZT sensors were glued on the two opposite sides of the cylindrical specimens using a two-component glue, in order to achieve a direct wave transmission to the specimen. To obtain comparable travel times through the different specimens the thickness of the glue layers should be the same for every specimen. This preparation of the sensor was achieved by the procedure presented in Fig. 4 and here described: (1) Two steel wedges with a thickness of 1.7 mm were temporarily fixed on a base steel plate. Then the glue was applied between these two wedges and the PZT sensor was placed on top of it. Thin paraffin films helped avoiding the steel wedges from becoming glued to the steel plate. (2) After the setting of the glue, the steel wedges were carefully removed from the plate, (3) as well as the sensor. Finally, the set composed by the PZT patch and the bottom glue layer (Fig. 5a) was directly attached

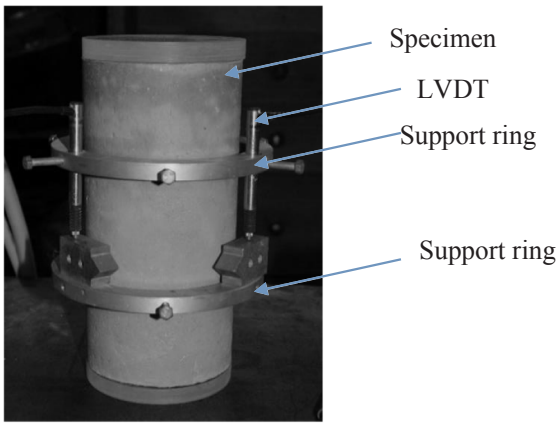

Fig. 1. Specimen with the deformation system for unconfined cyclic compression tests.

Fig. 2. Specimen and transducers during ultrasonic pulse velocity measurement.

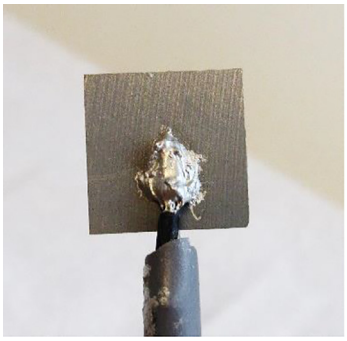

Fig. 3. PZT sensor with electric cable glued.

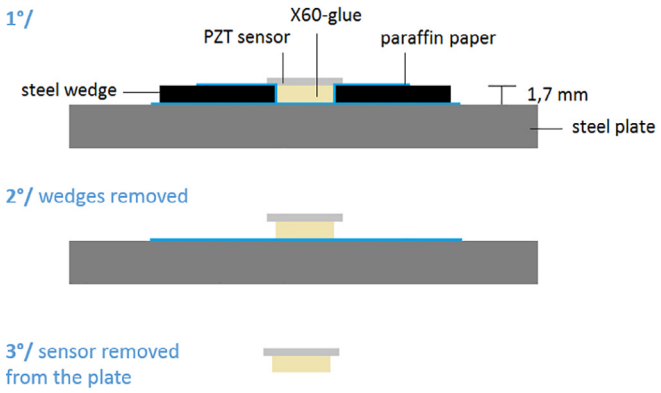

Fig. 4. Preparation of PZT sensors.

to the specimen and fixed/protected by covering it with an upper layer of glue (Fig. 5b).

A waveform generator – Rigol DG2041A [27] – was used to excite the transmitter transducer with a square pulse of 5 μs and an amplitude of 6.9 V. A digital oscilloscope – LeCroy 44Xi [28] – was used to read the signal of the receiver transducer. The travel time of the compression wave was evaluated in the time domain by determining the first wave deflection. Such determination was assisted by the Akaike Information Criterion (AIC) method [29].

EMM-ARM

The EMM-ARM mould adopted in this work consisted of a 580 mm long polyvinyl chloride (PVC; density = 1,200 kg m^{-3}; E-modulus = 3.4 GPa) tube with inner diameter of 47 mm and wall thickness of 1.5 mm (Fig. 6). After compaction of the mixture inside the mould, the extremities were closed with polystyrene caps. The mixture density was controlled by weighing the mould/mixture set. At 40 mm from the extremities of the mould, horizontal screws were used for support during testing, thus constituting a 500 mm span beam in simply supported conditions.

The data acquisition, resonant frequency determination and E-modulus estimation followed the same procedure presented by Silva et al. [25] which is briefly described below and schematically represented by Fig. 7. The measurement of the time series accelerations was made by piezoelectric accelerometers (PCB- frequency range of 0.15–1000 Hz, measurement range of ± 0.5 g, sensitivity of 10 V/g, resolution of 8 μg; 210 g of mass) fixed at mid span of the mould (as shown in Fig. 6b), connected to a data acquisition system (NI-USB-9234 DAQ, 24-bit) and recorded by a computer with a custom-made LabView code. The data was recorded at a sampling rate of 500 samples per second, in sets of 300 s, acquired at intervals of 900 s (Fig. 7a). The identification methodology for determination of the first resonant frequency of the testing beam, programed with MatLab functions, followed the Welch [30] procedure and the "peak-picking" method [31], that consisted in: dividing the time series signal in segments of 4096 points with an overlap of 50%; applying a signal processing window (Hanning) to the data segments; computing the autospectra of the windowed segments using the Fast Fourier Transform (FFT); and averaging the spectra associated with each time segment (Fig. 7b, c). With the identification of the first resonant frequency at each instant, it was possible to monitor its evolution with time (Fig. 7d). The resonant frequency of the beam was related with the E-modulus of the tested material by applying the dynamic equations of motion. For a simply supported beam with the first flexural resonant frequency f, free span L, uniformly distributed mass $\bar{m}$, and concentrated mass m_P at the mid-span (due to the existence of the accelerometer), and assuming stiff support conditions (infinite stiffness), the flexural stiffness of the composite beam EI (E standing for the E-modulus and I for the second moment of area of the composite cross-section) can be estimated using Eq. (2) [32].

$$2\cos(aL)(2\pi f)^2 m_P \sinh(aL) + \cos(aL)(2\pi f)^2 m_P \sinh(aL) - \cosh(aL)(2\pi f)^2 m_P \sin(aL) = 0,\ a = \sqrt[4]{(2\pi f)^2 \bar{m}/EI} \quad (2)$$

After determining the flexural stiffness of the composite beam (EI), the E-modulus of the studied material (E_{SL}) can be computed through application of Eq. (3), where E_M is the E-modulus of the mould material and I_M, I_{SL} are the second moments of area of the mould and of the soil-

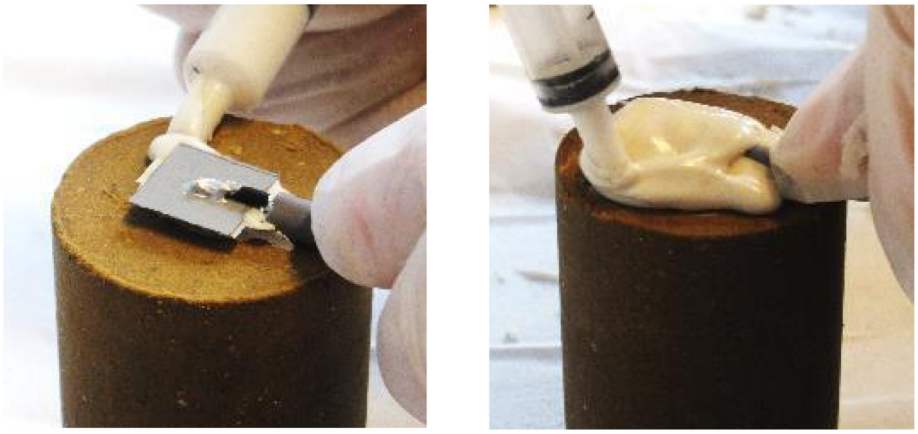

a) b)

Fig. 5. Attachment of the set PZT and glue layer to the specimen.

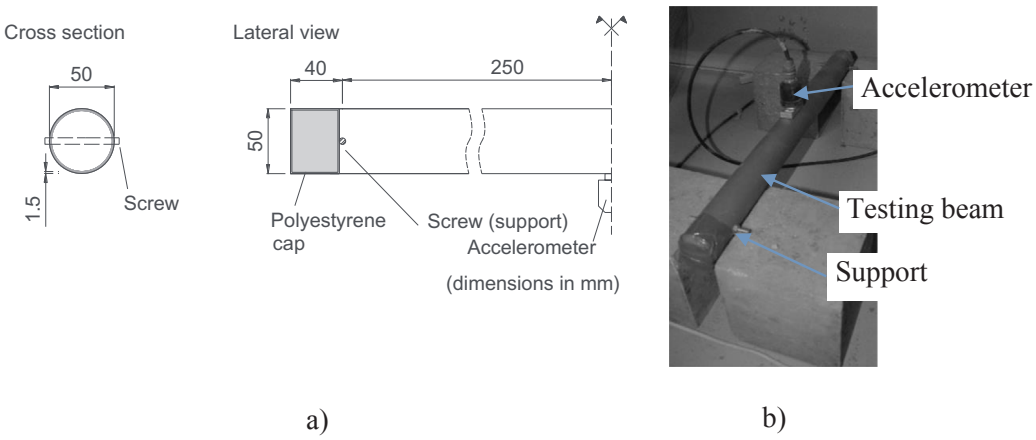

Fig. 6. EMM-ARM testing beam: (a) scheme with dimensions; (b) beam during testing.

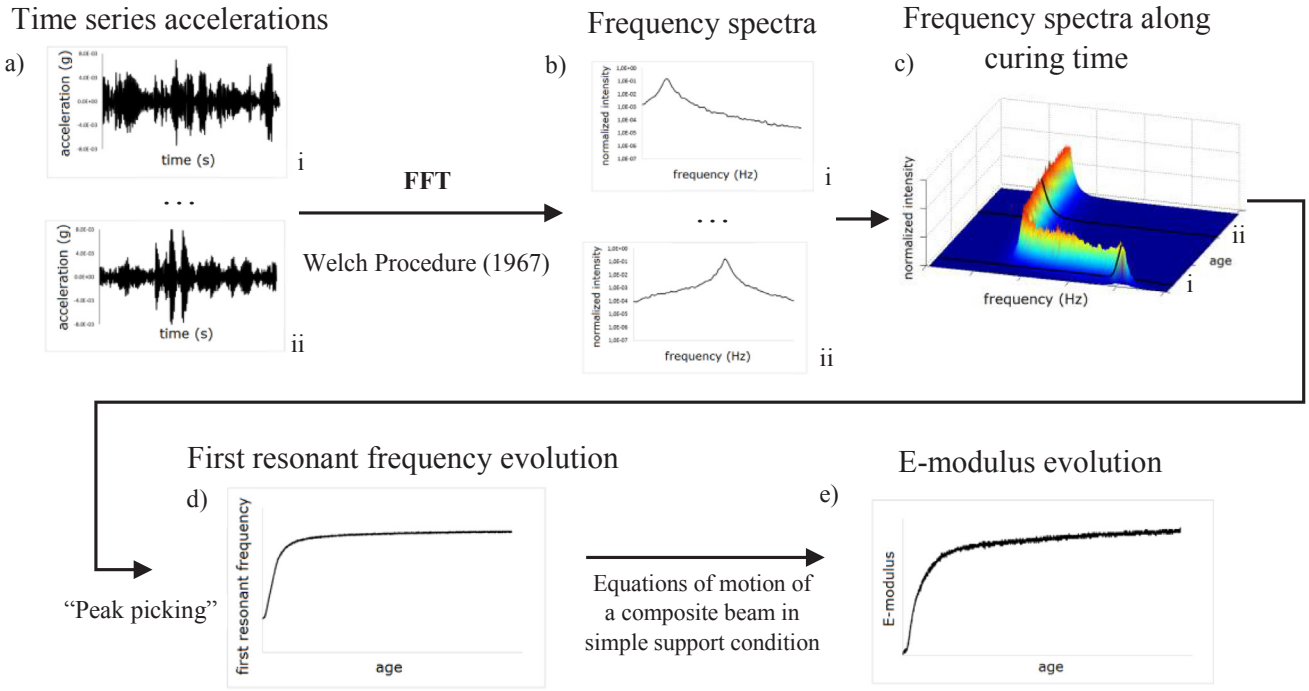

Fig. 7. EMM-ARM data processing.

lime mixture, respectively. The E-modulus *versus* time curve (Fig. 7e) can be then obtained by compiling the E_{SL} values obtained at each instant.

$$E_{SL} = (EI - E_M I_M)/I_{SL} \quad (3)$$

Evaluation of temperature effects

The method of equivalent age is widely used for estimation of the mechanical properties of cement based mixtures, such as concrete [33,34] and soil-cement [35]. This method takes into account the combined effects of time and temperature on the development of mechanical properties (such as strength or stiffness), and it is based on an adapted version of the Arrhenius' Law [33,34] presented on Eq. (4), where K is the reaction rate constant, A a proportional constant, E_a the apparent activation energy (J/mol), T the absolute temperature (K) and R the gas constant (8.314 J/(mol·K)).

$$K = A\exp[-E_a/(RT)] \quad (4)$$

However, the application of principles based on Arrhenius' law to the complex hydration reactions of binders such as cement or lime is an approximation, as the Arrhenius law was originally devised to describe the influence of temperature on the kinetics of simple chemical reactions. That is the reason why the adopted version of the Arrhenius law formulates the activation energy as being 'apparent'.

A good way of defining equivalent age consists in providing an example. Consider a given stabilised soil specimen cured for 10 days at a temperature of 30 °C, and tested for E-modulus. The Equivalent Age of this specimen corresponds to the age that a specimen of the same mixture, cured at a reference temperature, usually 20 °C, would take to attain the same E-modulus of the specimen cured at 30 °C. This equivalent age would, of course be higher than 10 days due to the thermal activated character of the binder hydration reactions (cement or lime, for example). One of the most popular models for equivalent age, based on the activation energy concepts, was proposed by Freiesleben Hansen and Pedersen [36]. It is presented on Eq. (5), where t_e is the equivalent age (days), T the curing temperature (K), T_{ref} the reference temperature (K), t the time period (days), and E_a and R are as previously defined.

$$t_e = \sum_0^t e^{[(Ea/R)((1/T)-(1/T_{ref}))]}\Delta t \quad (5)$$

Materials and specimens preparation

Materials

The soil used in this work consisted on a silt from Marche-Les-Dames (MLD) region on Belgium. It is composed of 52% of silt, 18% of clay and 30% of thin-grained sand, with a D50 (grain diameter at 50% passing in the grain size distribution) of about 30 µm. The Atterberg limits [37] were 20.1% for the plastic limit and 31.0% for the liquid limit and optimum dry density of 1844 kg/m^3 with an optimum water content of 15,1% determined by Standard Proctor test [38].

The soil was treated with a quicklime CL 90-Q [39] from Lhoist group, with the following particle size distribution: 98.9% < 0.5 mm and 84.1% < 90 µm.

Mixture proportioning and preparation

The mixture was prepared on a vertical axis mixer, with a 20 L capacity bowl, that operated with a planetary speed of 40 rpm and beater speed of 100 rpm. The mixture procedure starts by mixing the dried soil together with 3% of lime. The quantity of lime used was based on previous studies performed with MLD soil-lime mixtures [5,6]. Then, 5 min after turning on the mixer 19% of water is added and the mixer operates 5 more minutes. All the quantities (%) mentioned in the previous sentences were measured in terms of mass of dried soil. The mixture age counting starts at the instant when the water is added to the soil-lime mixture. After completing the mixture, the bowl is covered with plastic film in order to minimize water exchange with air, and preparation of specimens is done as quickly as possible.

Specimen preparation

In order to monitor the stiffness evolution of the soil-lime mixture, several specimens were prepared. The soil-lime mixture was compacted inside moulds with internal dimensions that corresponded to the intended dimensions for the specimens. All the specimens were prepared within an interval of 1 h since the start of the mixing process. The target wet bulk density of the mixture for all specimens was 1950 kg/m^3.

Table 1 presents the geometry, number and designation of specimens prepared to be used in each type of testing.

Results and discussion

Specimen densities

The bulk densities obtained for each specimen are presented in Table 2. The maximum variation observed was less than ± 1.5% when comparing to the target bulk density, which indicates a good performance during specimen preparation.

Table 2
Specimen bulk densities.

Type of testing	Specimen	Bulk density (kg/m^3)
PZT	PZT1	1955
	PZT2	1967
	PZT4	1962
EMM-ARM	EMM-ARM 20	1953
	EMM-ARM 30	1957
	EMM-ARM 40	1952
UCC	UCC1	1950
	UCC2	1940
US	US1	1977
	US2	1976
	US3	1944
	US4	1935

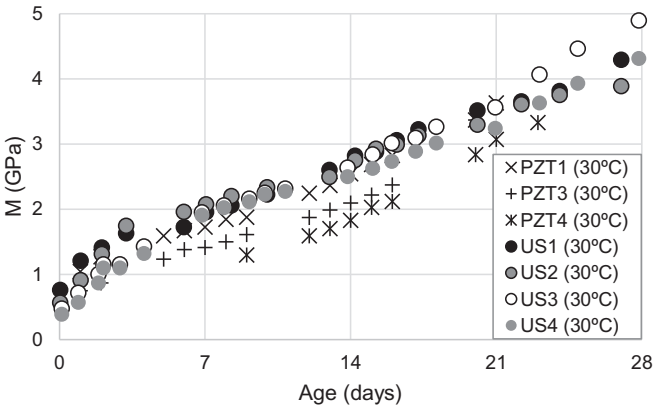

Fig. 8. M-modulus computed from US and PZT sensors on specimens cured at 30 °C.

Wave propagation based techniques (PZT and UPV)

The constrained modulus (M) values computed from the compression wave velocities measured with UPV and PZT sensors on specimens cured at 30 °C on the first 28 days of curing are presented in Fig. 8. The results obtained with the PZT sensors show a greater scatter than the results obtained with UPV sensors (US specimens), which can be related to the quality of the interface between the glue and the surface of the specimens. In fact, some decoupling was observed between the glue and specimens before 25 days of curing, probably due to a differential shrinkage phenomenon at the interface between the soil and the glue. This issue can be reduced by using a type of glue with more compatible behaviour with soil in terms of shrinkage. Some optimisation of the specimen dimensions should also be considered in future works in order to reduce the interaction with the specimen boundaries.

Despite the scatter observed, and taking into account that results were obtained in different laboratories, the results show a quite reasonable agreement between the two techniques, particularly on the

Table 1
Specimens characteristics.

Type of testing	Diameter (mm)	Length (mm)	Number of specimens	Curing temperatures (°C)	Designation
PZT (ULB)	36	71	3	30	PZT1, PZT2, PZT4
EMM-ARM (UM)	47	500	1	20	EMM-ARM 20
			1	30	EMM-ARM 30
			1	40	EMM-ARM 40
UCC (UM)	100	200	2	30	UCC1, UCC2
US (UM)	44	70	4	30	US1, US2, US3, US4

PZT: Piezoelectric transducers; EMM-ARM: Elasticity modulus measurement based on ambient response method; UCC: Unconfined cyclic compression; US: Ultrasonic pulse velocity; (UM): Universidade do Minho; (ULB): l'Université libre de Bruxelles.

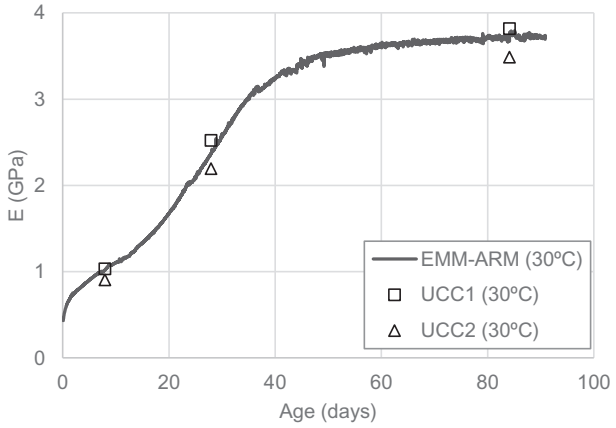

Fig. 9. E-modulus evolution obtained by EMM-ARM and UCC.

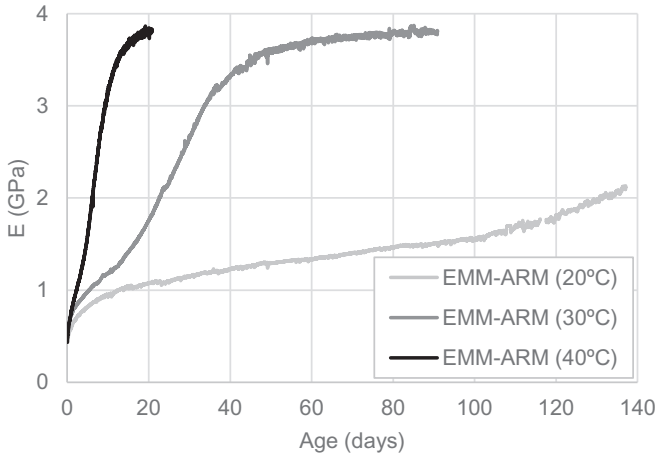

Fig. 10. E-modulus evolution obtained by EMM-ARM at temperatures of 20 °C, 30 °C and 40 °C.

PZT1 and the US specimens. This shows that there is a potential for using these low cost PZT sensors to monitor the stiffness evolution of treated soils. The results of Fig. 8 also allow to distinguish two different stages on the evolution of the M-modulus: the first occurs in the first 12 days of curing and the second after 12 days. This 2-staged stiffness evolution will be addressed in detail upon the interpretation of results obtained with EMM-ARM.

EMM-ARM and UCC

Fig. 9 presents the E-modulus evolution of the soil-lime mixture in the first 90 days of testing, under the curing temperature of 30 °C, obtained through EMM-ARM and UCC. An excellent coherence is observed between the results of EMM-ARM and UCC, which is a further confirmation of the reliability of EMM-ARM that has been reported/tested before several times [19]. When observing the E-modulus evolution obtained by EMM-ARM, it is evident that two different stages of the E-modulus evolution exist, as it had been observed in the results obtained with the wave based techniques shown in the previous section: the first stage starts immediately after compaction of the mixture, with a high rate of stiffness increase in the first hours followed by a continuous rate decrease until about 12 days age; the second stage starts about 12 days of age, with a new increase on the rate of stiffness up to about 37 days of age followed by a rate decrease until the end of the testing period around 90 days.

E-modulus evolution at temperatures of 20 °C, 30 °C and 40 °C

The E-modulus evolution of the soil-lime mixture cured at temperatures of 20 °C, 30 °C and 40 °C obtained by EMM-ARM testing are presented in Fig. 10. These results show that the increase of the curing temperature causes a significant increase of the rate of E-modulus evolution. As already observed for the curing temperature of 30 °C, it is also possible to identify the existence of two distinct stages on the E-modulus evolution curves of 20° and 40 °C. Due to the different nature of the reactions involved in the two stages, it may be also possible that they are probably being affected by temperature in different ways. According to such reasoning, the description of the kinetics of E-modulus evolution in stage 1 would be described with a distinct activation energy (Ea_1) than that of the second stage (Ea_2). This approach is developed in the next section by establishing a model that can be used to describe the evolution of E-modulus according to curing temperature, based on the equivalent age concept [36].

The two-stage kinetics evolution obtained with EMM-ARM at 20 °C is very similar to the results reported by De Bel et al. [6] regarding the evolution of compressive strength, that were obtained for the same mixture at 20 °C. De Bel et al. [6] observed a first stage that extended up to about 100 days of curing, the instant when the second stage started. They have also tested the soil-lime at several ages with X-ray diffraction (XRD), in order to monitor the mineral alterations and the appearance of new components resulting from soil treatment with lime. Those XRD tests revealed the production of calcium aluminate hydrates (CAH) during the first stage (up to 100 days), that may partly explain the increase in mechanical properties in such period. They also detected the presence of portlandite ($Ca(OH)_2$) and calcite ($CaCO_3$), indicating the presence of lime. In the second stage of evolution (> 100 days) the XRD peaks related to calcite had lower intensity and the portlandite peaks were no longer visible, meaning the lime had been almost completely consumed and suggesting the further evolution of the mechanical properties may result of different processes. One of such processes might be the structural rearrangement of the CAH throughout the further curing time. An alternative or concomitant explanation might rely on the reactions of the lime with the clay fraction, which could generate poorly crystallized CSH, and therefore having no distinct diffraction peaks.

Modelling of experimental data

Eq. (6) can be used as a best-fit mathematical model to describe the E-modulus (E) evolution of a curing mixture (e.g. concrete or soil-cement), as function of age (t). This equation proposed by Silva et al. [25] results of the combination of Eq. (7) [40], that describes the evolution of the degree of reaction/hydration as a function of time, and Eq. (8) [34] that describes the evolution of E-modulus as a function of the degree of reaction/hydration. In these equations, α is the degree of hydration, α_0 is the degree of hydration of the binder at the instant of setting (for stabilized soils $\alpha_0 = 0$ as it has initial stiffness), E_1 is the hypothetic value of E when $\alpha = 1$, (α_u) is the ultimate degree of hydration, β is a hydration shape parameter, τ is a hydration time parameter and a is a constant ($a = E_1 \times \alpha_u^{(1/2)}$). In the scope of cement-based materials, Schindler and Folliard [34] have demonstrated that the parameters a and β are temperature independent, whereas τ is temperature dependent. The same assumption is made in this work.

$$E(t) = a \times e^{\left[-\frac{1}{2}\times(\tau/t)^{\beta}\right]} \quad (6)$$

$$E(\alpha) = E_1 \times [(\alpha - \alpha_0)/(1 - \alpha_0)]^{1/2} \quad (7)$$

$$\alpha(t) = \alpha_u \times e^{[-(\tau/t)^{\beta}]} \quad (8)$$

Even though Eq. (6) is appropriated to fit the typical "S" shape evolution found on the cement-based mixtures [15], it is definitely not suitable to integrally describe the two sequential "S" shapes observed in experimental E-modulus curves shown in Fig. 10. Assuming that the E-modulus E(t) of the soil-lime mixture results of the initial E-modulus of the mixture E_0 and the combined stiffness contribution of reactions

Table 3
Parameters of the model (Eq. (10)) fitting to the experimental results.

T (°C)	20	30	40
a_{r1} (GPa)	2.91		
β_{r1}	0.25		
a_{r2} (GPa)	2.15		
β_{r2}	3.13		
τ_{r1}	1514.94	477.82	138.36
τ_{r2}	189.82	30.78	8.23
$E0$ (GPa)	0.413	0.450	0.547

initiated on stage 1 and reactions initiated on stage 2 ($E_{r1}(t)$ and $E_{r2}(t)$ respectively), then $E(t)$ can be described by Eq. (9). Thus, assuming that E_{r1} and E_{r2} can be individually fitted by Eq. (6), then Eq. (9) takes the form presented on Eq. (10), where indexes 1 and 2 identify that the corresponding parameter is related to the reactions of stage 1 and 2, respectively.

$$E(t) = E_0 + E_{r1}(t) + E_{r2}(t) \tag{9}$$

$$E(t) = E_0 + a_{r1}e^{\left[-\frac{1}{2}(\tau_{r1}/t)^{\beta r1}\right]} + a_{r2}e^{\left[-\frac{1}{2}(\tau_{r2}/t)^{\beta r2}\right]} \tag{10}$$

Table 3 presents the parameters of Eq. (10) determined by fitting the experimental E-modulus results obtained at curing temperatures of 20 °C, 30 °C and 40 °C using the least squares method and making the parameters a and β equal for all the different temperatures. Fig. 11 displays the values obtained with Eq. (10) and the experimental data, showing that excellent coherences can be obtained for all tested temperatures ($R^2 > 0.9$ in all cases). It is remarkable to notice that these coherences were attained with a single temperature dependent parameter for each reaction (τ_1 and τ_2).

Apparent activation energy estimation

Replacing t in Eq. (10) by the equivalent age (Eq. (5)), and separating the contribution of each reaction, it is possible to obtain Eq. (11) that allows to express E_{ri} (E-modulus contribution of reaction i) taking into account the Ea_i (apparent activation energy of reaction i), the temperature history and the parameters a_{ri},τ_{ri} and β_{ri}.

$$E_{ri}(t) = a_{ri}e^{\left[-\frac{1}{2}\left(\tau_{ri}/\left(\sum_0^t e^{[(Ea_i/R)((1/T)-(1/T_{ref}))]\Delta t}\right)\right)^{\beta_{ri}}\right]},\ i = \{1, 2\} \tag{11}$$

The values of parameters a_{ri},τ_{ri} and β_{ri} for 20 °C (293.15 K), presented in Table 3 were applied to Eq. (11), and the activation energy of reactions (1) and (2) (Ea_1 and Ea_1) were estimated through the least square method, as to match the fitted results of E_{r1} and E_{r2} for 30 °C and 40 °C (determined using parameters of Table 3).

This procedure is similar to the superposition method described by Geoffroy [41]. The values for the apparent activation energies that gives the best fit were Ea_1 = 89 929 J/mol and Ea_2 = 128 006 J/mol

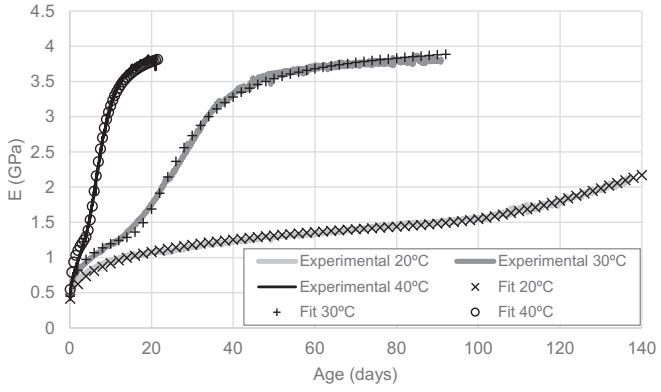

Fig. 11. Model fitting to EMM-ARM experimental results at temperatures of 20 °C, 30 °C and 40 °C.

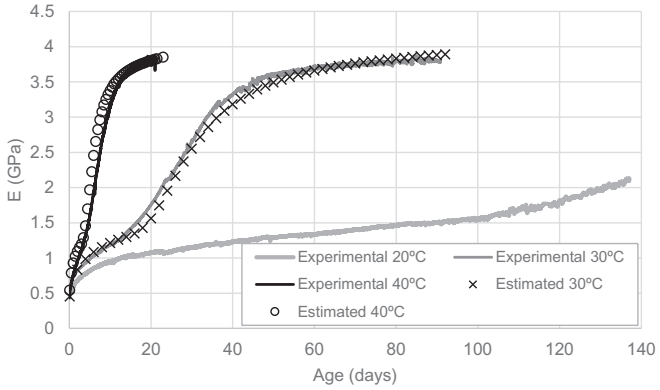

Fig. 12. Estimation of E-modulus evolution at temperatures of 30 °C and 40 °C from the 20 °C data.

($R^2 > 0.9$ in all cases). These values of Ea are much higher than those that are usually observed in cementitious materials, which typically are around 40 000 J/mol [42]. This means the reactions involved are more sensitive to the curing temperatures than cement-based materials.

Through application of Eqs. (11) and (5), using the reference temperature of 20 °C and respective parameters in Table 3, as well as the above calculated activation energies, it was possible to estimate the E-modulus evolution at temperatures of 30 °C and 40 °C. Fig. 12 shows the comparison between the estimated values and the experimental results demonstrating the validation of the methodology used to calculate the two constant apparent activation energies for the two types of reactions involved in the curing of this soil-lime mixture.

Conclusions

The stiffness evolution of a silt soil stabilized with quicklime cured at 30 °C is initially presented on this paper, with results obtained through 3 distinct methodologies: (i) two different wave based techniques, namely PZT and UPV (piezoelectric transducers and ultrasonic pulse velocity, respectively); (ii) UCC (unconfined cyclic compression testing) and; (iii) EMM-ARM (Elasticity Modulus Measurement through Ambient Response Method).

A good coherence of M-modulus values determined with PZT and UPV sensors was observed. However, the results obtained with PZT show a higher scatter than the results obtained with the UPV. Despite this, PZT sensors have the advantage of their low cost, justifying further research in the context of geomaterials.

A very good coherence was observed when comparing the EMM-ARM results with the E-modulus determined with classical UCC testing, at curing temperature of 30 °C, confirming the validity of EMM-ARM.

The results obtained by the different methodologies (PZT, UPV, EMM-ARM and UCC) at 30 °C and further EMM-ARM tests at temperatures of 20 °C and 40 °C, all revealed two different stages on the stiffness evolution suggesting the existence of two different chemical phenomena involved. Based on the previous work of De Bel et al. [6] with same mixture is believed that the E-modulus evolution in the first stage seems to be mostly related to the formation of calcium aluminate hydrates (CAH). However, the E-modulus evolution in the second stage can be more related to a structural rearrangement of CAH and the formation of calcium silicate hydrates (CSH).

These two distinct stages involved in the evolution of E-modulus with time suggest the existence of two apparent activation energies (one for each process). For this purpose, an approach involving a decomposition of a mathematical model fitted to the experimental data in the contribution of two process was proposed. The apparent activation energies estimated where 89 929 J/mol and 128 006 J/mol for the reactions initiated on stage 1 and reactions initiated on stage 2, respectively. These values are higher than those found for other type of

cementitious materials, such as concrete, and means that the reactions involved are much more sensitive to the curing temperature. Despite the different kinetics observed, the results obtained, particularly at 30 °C and 40 °C, suggest that the long term E-modulus will tend to the same value, regardless of the curing temperature.

The findings of this work show the potential of using EMM-ARM allied to the proposed methodology for activation energy estimations, helping to understand the curing process on stiffness kinetics of complex materials as soil-lime mixtures. This can bring important benefits in laboratory studies, were soil-lime curing is frequently accelerated by raising temperature, and in evaluating stabilized layers in field, considering the temperature effects in stiffness predictions. Indeed, the developed laboratory experimental procedure and interpretation is deemed to be also applied properly in outdoor conditions where the temperature is not constant.

Acknowledgements

Funding provided by the Portuguese Foundation for Science and Technology (FCT) to the Research Project IntegraCrete PTDC/ECM-EST/1056/2014 (POCI-01-0145-FEDER-016841), as well as to the Research Unit ISISE (POCI-01-0145-FEDER-007633) is gratefully acknowledged.

References

[1] Little DN, Scullion TKPBJ. Identification of the structural benefits of base and subgrade stabilization. Res. Rep. 1287-2F. Texas Transp. Inst.; 1994.
[2] Puppala A, Mohammad L, Allen A. Engineering behavior of lime-treated Louisiana subgrade soil. Transp Res Rec 1996;1546:24–31. https://doi.org/10.3141/1546-03.
[3] Gomes Correia A, Winter MG, Puppala AJ. A review of sustainable approaches in transport infrastructure geotechnics. Transp Geotech 2016;7. https://doi.org/10.1016/j.trgeo.2016.03.003.
[4] Jauberthie R, Rendell F, Rangeard D, Molez L. Stabilisation of estuarine silt with lime and/or cement. Appl Clay Sci 2010;50:395–400. https://doi.org/10.1016/j.clay.2010.09.004.
[5] Verbrugge J-C, De Bel R, Correia AG, Duvigneaud P-H, Herrier G. Strength and micro observations on a lime treated silty soil. Road mater. new innov. pavement eng. Reston, VA: American Society of Civil Engineers; 2011. p. 89–96. https://doi.org/10.1061/47634(413)12.
[6] De Bel R, Gomes Correia A, Duvigneaud P-H, Francois B, Herrier G, Verbrugge J-C. Long-term mechanical and physico-chemical evolution of silty soil treated with lime. Colloq TerDOUEST 2013. 2013.
[7] Bell FG. Lime stabilization of clay minerals and soils. Eng Geol 1996;42:223–37. https://doi.org/10.1016/0013-7952(96)00028-2.
[8] Al-Mukhtar M, Khattab S, Alcover J-F. Microstructure and geotechnical properties of lime-treated expansive clayey soil. Eng Geol 2012;139–140:17–27. https://doi.org/10.1016/j.enggeo.2012.04.004.
[9] Okyay US, Dias D. Use of lime and cement treated soils as pile supported load transfer platform. Eng Geol 2010;114:34–44. https://doi.org/10.1016/j.enggeo.2010.03.008.
[10] Lemaire K, Deneele D, Bonnet S, Legret M. Effects of lime and cement treatment on the physicochemical, microstructural and mechanical characteristics of a plastic silt. Eng Geol 2013;166:255–61. https://doi.org/10.1016/j.enggeo.2013.09.012.
[11] Negawo WJ, Di Emidio G, Bezuijen A, Verastegui Flores RD, François B. Lime-stabilisation of high plasticity swelling clay from Ethiopia. Eur J Environ Civ Eng 2017. https://doi.org/10.1080/19648189.2017.1304272.
[12] Rajasekaran G. Sulphate attack and ettringite formation in the lime and cement stabilized marine clays. Ocean Eng 2005;32:1133–59. https://doi.org/10.1016/j.oceaneng.2004.08.012.
[13] Millogo Y, Hajjaji M, Ouedraogo R. Microstructure and physical properties of lime-clayey adobe bricks. Constr Build Mater 2008;22:2386–92. https://doi.org/10.1016/j.conbuildmat.2007.09.002.
[14] ASTM-C593-06. Standard specification for fly ash and other pozzolans for use with lime for soil stabilization. Am Soc Test Mater 2011;06:1–5. https://doi.org/10.1520/C0593-06R11.
[15] Azenha M, Ramos LF, Aguilar R, Granja JL. Continuous monitoring of concrete E-modulus since casting based on modal identification: a case study for in situ application. Cem Concr Compos 2012;34:881–90. https://doi.org/10.1016/j.cemconcomp.2012.04.004.
[16] Azenha M, Ferreira C, Silva J, Correia AG, Aguilar R, Ramos LF. Continuous stiffness monitoring of cemented sand through resonant frequency. Emerg. technol. mater. des. rehabil. insp. roadw. pavements Reston, VA: American Society of Civil Engineers; 2011. p. 174–83. https://doi.org/10.1061/47629(408)22.
[17] Silva J, Azenha M, Correia AG, Ferreira C. Continuous stiffness assessment of cement-stabilised soils from early age. Géotechnique 2013;63:1419–32. https://doi.org/10.1680/geot.13.P.021.
[18] Silva J, Azenha M, Correia AG, Granja J. Continuous monitoring of sand-cement stiffness starting from layer compaction with a resonant frequency-based method: issues on mould geometry and sampling. Soils Found 2014;54. https://doi.org/10.1016/j.sandf.2013.12.006.
[19] Azenha M, Silva J, Granja J, Gomes-Correia A. A retrospective view of EMM-ARM: application to quality control in soil-improvement and complementary developments. Procedia Eng 2016;143. https://doi.org/10.1016/j.proeng.2016.06.043.
[20] Correia AG. Evaluation of mechanical properties of unbound granular materials for pavements and rail tracks. In: Gomes Correia A, Loizos A, editors. Geotech. pavement railw. des. constr. Rotterdam: Millpress; 2004. p. 35–60.
[21] Gomes Correia A, Reis Ferreira SM, Faria Araújo N. Precision triaxial tests to determine deformability characteristics [in Portuguese]. 10 Congr. Nac. Geotec. vol. 2. Lisbon: Sociedade Portuguesa de Geotecnia; 2006. p. 317–26.
[22] Gomes Correia A, Martins J, Caldeira L, Maranha das Neves E, Delgado J. Comparison of in situ performance-based tests methods to evaluate moduli of railway embankments. Bearing Capacity of Roads, Railways and Airfields. Al-Qadi T, editor. 8th Int. conf. vol. 1. Unversity of Illinois, Champaign, Illinois, USA: Taylor & Francis Group; 2009. p. 1331–40.
[23] Biarez J, Gomes Correia A, Lopez-Caballero F. From very small strains to failure. Deform. charact. geomaterials recent investig. prospect. 2005. p. 125–41.
[24] Amaral MF, Viana da Fonseca A, Arroyo M, Cascante G, Carvalho J. Compression and shear wave propagation in cemented-sand. Géotech Lett 2011;1:79–84.. https://doi.org/10.1680/geolett.11.00032.
[25] Silva J, Azenha M, Correia AG, Ferreira C. Continuous stiffness assessment of cement-stabilised soils from early age. Geotechnique 2013;63. https://doi.org/10.1680/geot.13.P.021.
[26] Poceq. Ultrasonic Pulse Velocity – Pundit Lab 2014; 2014. http://www.proceq.com/en/non-destructive-test-equipment/concrete-testing/ultrasonic-pulse-velocity/pundit-lab.html?pqr=17.
[27] Rigol. DG2041A-Arbitrary Waveform Function Generator; 2014. http://www.rigolna.com/products/waveform-generators/dg2000/dg2041a/.
[28] TeledyneLecroy. WaveRunner Xi – A Series 2014; 2014. http://cdn.teledynelecroy.com/files/pdf/waverunner_xi-a_datasheet.pdf.
[29] Akaike H. Information theory as an extension of the maximum likelihood principle. Second int symp inf theory. 1973. p. 267–81.
[30] Welch P. The use of fast Fourier transform for the estimation of power spectra: a method based on time averaging over short modified periodograms. IEEE Trans Audio Electro-Acoust 1967;15:70–3. https://doi.org/10.1109/tau.1967.1161901.
[31] Ewins DJ. Modal testing: theory, pratice and application. 2nd ed.; 2000.
[32] Azenha M, Magalhães F, Faria R, Ramos L, Cunha Á. Mesurement of concrete E-modulus evolution since casting: a novel method based on ambient vibration. Cem Concret Res 2010;40:1096–105.
[33] Weiss J, Berke N. Shrinkage reducing admixtures. vol. Report of; 2002.
[34] Schindler AK, Folliard KJ. Heat of hydration models for cementitious materials. ACI Mater J 2005;101:24–33.
[35] Chitambira B, Al-Tabbaa A, Perera ASR, Yu XD. The activation energy of stabilised/solidified contaminated soils. J Hazard Mater 2007;141:422–9. https://doi.org/10.1016/j.jhazmat.2006.05.080.
[36] Freiesleben Hansen P, Pedersen J. Maturity computer for controlled curing and hardening of concrete. Nord Betong 1977;1:19–34.
[37] AFNOR. NF P 94-051 – Determination des Limites d'Atterberg; 1993.
[38] AFNOR. NF P 94-093 – Sols: Reconnaissance et essais – Détermination des références de compactage d'un matériau – Essai Proctor Normal – Essai Proctor modifié; 1999.
[39] CEN. EN 459-1 – Building lime – part 1: definitions, specifications and conformity criteria; 2010.
[40] Rostásy F, Gutsch A, Krauß M. Computation of stresses and cracking criteria for early age concrete – methods of iBMB; 2001.
[41] Geoffroy J-M. Résultats et recommandations du projet national Calibé – La maîtrise de la qualité du béton. Paris: Presses des Ponts et Chaussées; 2004.
[42] Azenha M. Numerical simulation of the structural behaviour of concrete since its early ages [PhD. Thesis]. Faculty of Engineering of the University of Porto; 2009.